Green Chemistry

PAPER

View Article Online
View Journal | View Issue



Cite this: *Green Chem.*, 2022, **24**, 3689

# A molecular motor from lignocellulose†

Thomas Freese, ‡[a] Bálint Fridrich, ‡[a] Stefano Crespi, §[a] Anouk S. Lubbe,[a] Katalin Barta *[a,b] and Ben L. Feringa *[a]

Received 21st January 2022,
Accepted 11th March 2022

DOI: 10.1039/d2gc00291d

rsc.li/greenchem

Lignin is the largest natural source of functionalized aromatics on the planet, therefore exploiting its inherent structural features for the synthesis of aromatic products is a timely and ambitious goal. While the recently developed lignin depolymerization strategies gave rise to well-defined aromatic platform chemicals, the diversification of these structures, especially toward high-end applications is still poorly addressed. Molecular motors and switches have found widespread application in many important areas such as targeted drug delivery systems, responsive coatings for self-healing surfaces, paints and resins or muscles for soft robotics. They typically comprise a functionalized aromatic backbone, yet their synthesis from lignin has not been considered before. In this contribution, we showcase the synthesis of a novel light-driven unidirectional molecular motor from the specific aromatic platform chemical 4-(3-hydroxypropyl)-2,6-dimethoxyphenol (dihydrosynapyl alcohol) that can be directly obtained from lignocellulose *via* a reductive catalytic fractionation strategy. The synthetic path takes into account the principles of green chemistry and aims to maintain the intrinsic functionality of the lignin-derived platform molecule.



## Introduction

Lignin serves as a renewable source of sustainable aromatic products. Recently, several efficient lignin depolymerization strategies have been developed, giving rise to aromatic platform chemicals with high yields and selectivity.[1,2] Methods relying on stabilization strategies both during pulping as well as depolymerization have resulted in well-defined aromatics and suppression of undesired recondensation phenomena.[3] Among these, reductive catalytic fractionation (RCF) has proven especially effective.[4,5] During RCF, lignocellulose fractionation is performed in conjunction with native lignin depolymerization using a metal catalyst in reductive atmosphere and allows obtaining propyl- or propanol-guaiacols and syringols with high selectivity, depending on conditions. The conversion of these platform chemicals to drop-in intermediates such as BTX[6] or phenol[7] or to bio-based polymer building blocks, such as bisphenols has already been investigated.[8] Interestingly, much less attention was devoted to the conversion of these molecules to fine chemicals[9] or products with a specific function and more specialized applications.[10,11]

We have previously described the use of copper doped porous metal oxides ($Cu_{20}$PMO) in the reductive catalytic fractionation of hardwood and softwood as starting materials, delivering dihydroconiferyl alcohol or dihydrosinapyl alcohol from softwood and hardwood species, respectively.[12] The diversification of dihydroconiferyl alcohol to a wide range of valuable building blocks, including amines has also been demonstrated.[12] One of these specific value-added compounds was the indanone derivative (5,6-dimethoxy-1-indanone) that is a crucial intermediate in the synthesis of the anti-Alzheimer's drug Donepezil. Interestingly, we used similar indanones as common starting materials to design unidirectional molecular rotary motors and switches[13–20] and established applications such as dynamic surface wettability or rotating a macroscopic object on top of a liquid crystal surface.[21–23] In order to perform work a molecular motor or switch has to be interfaced with its surrounding environment.[24]

Motion can be harnessed by attaching molecular motors on a surface or incorporating them into an ordered bulk material such as polymers, liquid crystals or supramolecular systems, taking advantage of the amplification over different length scales of the (supra-) molecular ordered motors.[23,25–29]

Prominent challenges are found in systems chemistry where the structural modifications at the molecular level that are typical of switches and motors must translate to the other components of a complex molecular system. This motion communication leads to a change in assembly or in the chemical

[a]*Stratingh Institute for Chemistry, University of Groningen, Nijenborgh 4, 9747 AG Groningen, The Netherlands. E-mail: b.l.feringa@rug.nl*
[b]*Department of Chemistry, Organic and Bioorganic Chemistry, University of Graz, Heinrichstrasse 28/II, 8010 Graz, Austria. E-mail: katalin.barta@uni-graz.at*

†Electronic supplementary information (ESI) available. CCDC 2127292 and 2127293. For ESI and crystallographic data in CIF or other electronic format see DOI: https://doi.org/10.1039/d2gc00291d

‡These authors contributed equally to this work.

§Current address: Department of Chemistry, Ångström Laboratory, Uppsala University, Box 523 75120 Uppsala, Sweden.

environment that can be used for various applications.[30] For instance, incorporating switches enabled us to design new responsive materials capable of exerting a dynamic function upon light irradiation or redox reactions.[31–33] By incorporating switching functionalities into amphiphiles or small-molecule gelators, one can gain control over their supramolecular aggregates, leading to future potential applications, such as targeted drug delivery systems, responsive coatings for self-healing surfaces, paints and resins or muscles for soft robotics.[24,28,34] In general, incorporation of molecular switches enables the dynamic control of function of materials from the nano-, meso- and micro- to macroscopic level.[24] Consequently, synthesizing a motor core possessing handles that allows functionalisation in a late-stage step will introduce modularity for potential applications.

In our endeavour to unlock the potential of chemicals sourced from biomasses and facing these fascinating opportunities for molecular machines and responsive materials, we attempted to develop a synthetic strategy that allows access to novel molecular motors, directly from the native lignin component of wood sawdust, while considering and whenever possible, implementing the main principles of Green Chemistry.[35] This work represents the first molecular motor obtained from non-edible, renewable resources as an innovative high value target molecule with a specific function (see Fig. 1).

## Results and discussion

In 1999 our group designed the first molecular motor able to undergo unidirectional 360° rotation powered by light.[13] In the following years we developed a library of overcrowded alkenes by connecting two identical halves *via* a double bond functioning as rotary axle, which featured *E*,*Z*-geometrical isomers and

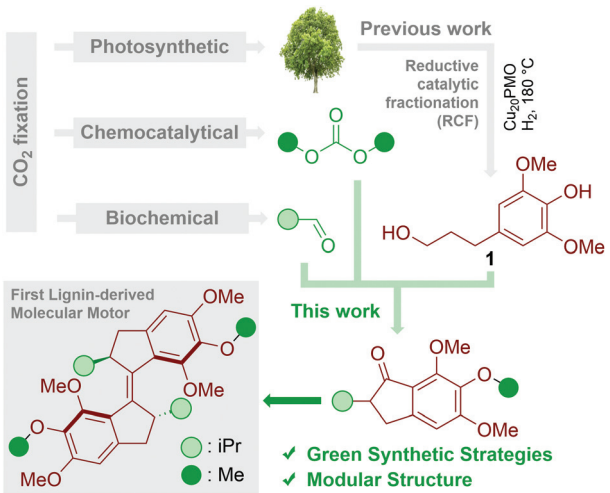


Fig. 1 Schematic representation of the design and route to the first wood-based light-driven molecular motor representing a complex functional molecule.

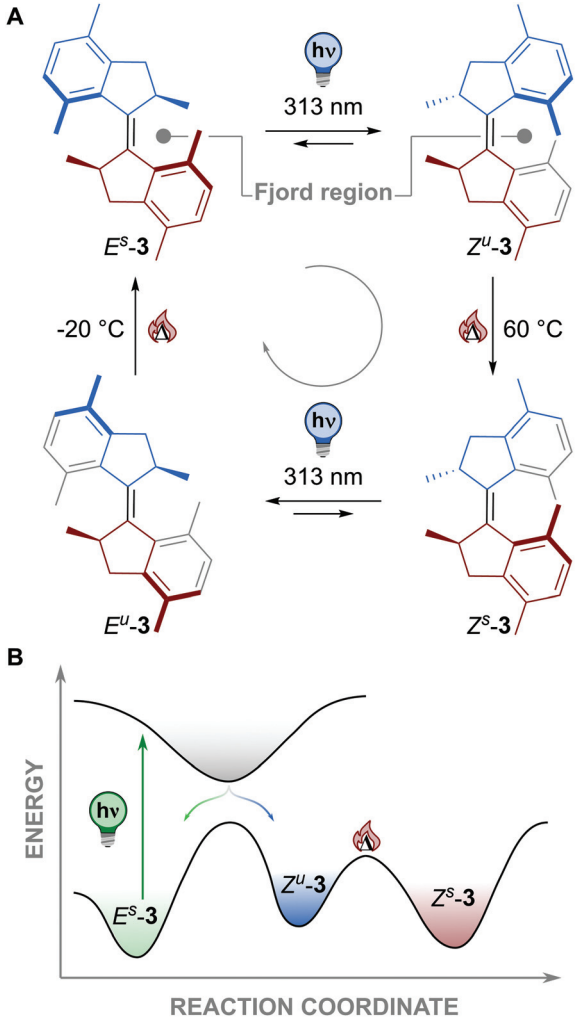


Fig. 2 (A) Four state rotary cycle of a first generation motor based on an overcrowded alkene.[36] (B) Energy profile of the first 180° rotation of a first generation molecular motor.

two chiral elements *i.e.* stereogenic centres and helical chirality ($E^s$-**3** in Fig. 2).[36] The steric crowding in the *fjord* region resulted in the molecule assuming a folded structure, with the two methyl substituents adopting preferentially pseudo-axial orientation, thus imparting helical chirality to the molecule. These unique features and the stiff-stilbene-type photoisomerization prime the directionality of the rotation about the double bond (the rotary axle). A full 360° rotation consists of four steps: two photochemically and two thermally activated ones.

Irradiation of $E^s$-**3** in Fig. 2 with UV light (313 nm) triggers the *E*-to-*Z* isomerisation about the double bond, resulting in the formation of $Z^u$-**3**, characterized by opposite helical chirality. This photoisomerization step is reversible and, under continuous irradiation, a photostationary state (PSS) is ultimately reached, with a distribution of the $Z^u$ to $E^s$ isomers of 1 : 1.1.[36] $Z^u$-**3** assumes a twisted geometry with the methyl substituents in pseudo-equatorial position, which is energetically less

 

favoured (Fig. 2B). Thus, this photogenerated and energetically uphill reaction builds-up strain, which is released in the subsequent thermal step. A thermal helix inversion (THI) occurs, reverting the helicity of the molecule, to obtain the folded $Z^s$-**3**. Both halves slide past each other, resulting in a more energetically favoured pseudo-axial position for the methyl substituents. The unidirectional 180° rotation is completed by this energetically downhill process, which is effectively withdrawing the higher-energy isomer $Z^u$-**3** from the photochemical equilibrium. The second half of the full (360°) rotary cycle involves again a sequential photochemical and thermal step: Photoisomerization results in the twisted structure of $E^u$-**3** (PSS *E*-to-*Z* ratio 1 : 8), with the methyl substituents in pseudo-equatorial position, and completion of the full 360° rotation cycle by THI back to $E^s$-**3**.[37]

We started the project by evaluating possible molecular motor-like structures that could be generated from the molecules originating from RCF of lignocellulose over $Cu_{20}$PMO, namely dihydroconiferyl and dihydrosinapyl alcohol. Our previously developed method using $Cu_{20}$PMO allows operating at lower temperatures during RCF compared to most methods, thus maintaining the primary alcohol in these platform chemicals. This functionality is essential for further oxidation and cyclization to the corresponding indanone derivative, as we have previously demonstrated by using pine lignocellulose.[12] First generation molecular motors are commonly synthesized by homocoupling of such functionalized indanones.[19] Substituents in the alpha and *ortho* positions to the ketone functionality are required to ensure the unidirectionality of the target compound. Moreover, based on a previous study, a methoxy group in the *fjord* region is expected to lead to a faster unidirectional movement compared to a methyl substituent.[38] It is also necessary to introduce a substituent in the alkyl position adjacent to the ketone in order to introduce a stereogenic centre and thus ensure unidirectionality of the rotation.

To our delight, these requirements can be fulfilled by starting from dihydrosinapyl alcohol **1** (Fig. 1) which is typically the main product of RCF of hardwood rich in S units.[12] In our previous work, the reductive catalytic fractionation of the hardwood species poplar, beech and maple delivered above 30% monomer yield, with **1** as the main product.[12] This provides access to the indanone structure to be sourced only from renewables. Furthermore, interestingly, the isobutyraldehyde moiety can also be made in principle bio-derived[39] and the phenol methylation can be carried out using the green methylating agent dimethyl carbonate,[40] another reactant accessible from renewable (Fig. 1). We envisioned that the additional methoxy substituents in target motor **7**, which are directly provided by the inherent structure of the lignin backbone, would result in a higher electron density, that may impart a bathochromic shift of the absorption spectrum, a major challenge in the field of molecular machines.[19]

## Synthetic strategy

The preparation of motor **7** (Scheme 1) started from dihydrosinapyl alcohol **1**, which could easily be obtained in one step from hardwood sawdust by treatment with a non-precious

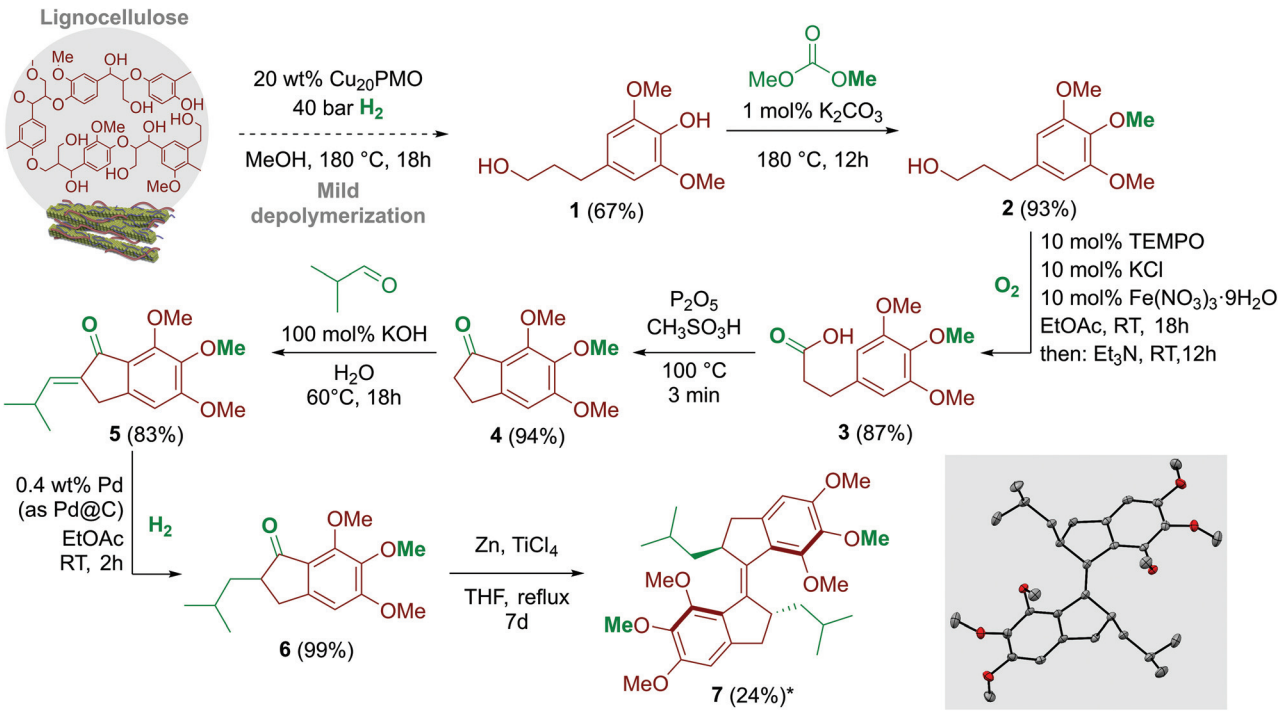


**Scheme 1** Synthesis route for compound **7** (*yield based on recovered starting material). Dashed line represents our previous work.[12] For detailed experimental section see ESI.† In the inset: molecular structure of compound *E* (*R*,*R*)-**7** (50% probability ellipsoids; hydrogen atoms are omitted for clarity).

metal catalyst, copper-doped porous metal oxide ($Cu_{20}$PMO), under reductive atmosphere (40 bar $H_2$) at 180 °C in methanol.[12] It is also possible to source the same compound with very high yield and selectivity by relying on the aldehyde assisted fractionation (AAF) of poplar lignocellulose, using propionaldehyde as stabilizing agent, followed by reductive depolymerization over Ni catalysts.[41] The selective methylation of the phenol moiety of **1** with dimethyl carbonate (DMC) as a potentially renewable, environmentally benign, low-toxic methylating agent and solvent[42] provided the trimethoxy compound **2** (93% yield). The oxidation of **2** to 3-(3,4,5-trimethoxyphenyl)propanoic acid **3** was realized at room temperature with oxygen (atmospheric pressure) as oxidant, with a catalytic system consisting of $Fe(NO_3)_3{\cdot}9H_2O$, KCl and TEMPO, with a yield of 87%.[43] For the oxidation, ethyl acetate (EtOAc) was used as a benign alternative to 1,2-dichloroethane (DCE), which is commonly used in similar oxidation procedures.[43] The product was isolated with pH selective extraction instead of solvent intense column chromatography, exploiting the solubility difference of the sodium salt and the free acid of the (trimethoxyphenyl)propanoic acid **3** in diethyl ether (discussed in detail in the ESI†). **3** can be alternatively obtained by the hydrogenation of (*E*)-3-(3,4,5-trimethoxy)cinnamic acid (**0**, see ESI†). Acid **3** was cyclized in three minutes with Eaton's reagent ($P_2O_5$, $CH_3SO_3H$)[44] at 100 °C to yield 5,6,7-trimethoxy-2,3-dihydro-1*H*-inden-1-one **4**. The crucial stereogenic centre was introduced in two steps. First, the aldol condensation of **4** with isobutyraldehyde in water at 60 °C yielded the corresponding olefin 5,6,7-trimethoxy-2-(2-methylpropylidene)-2,3-dihydro-1*H*-inden-1-one **5**. After standard workup, the crude product was purified by precipitation with 83% isolated yield. Next, a clean and simple procedure for the double bond hydrogenation in **5** was developed using 1 mol% Pd@C at room temperature and 1 bar pressure of $H_2$ in ethyl-acetate. The desired 2-isobutyl-5,6,7-trimethoxy-2,3-dihydro-1*H*-inden-1-one **6** was obtained in quantitative yield. Finally, the central double bond in overcrowded alkene **7** was constructed *via* McMurry homocoupling, providing the desired compound in 16% yield (24% based on recovered starting material). The new molecular motor was obtained from lignin derived **1** in an overall yield of 15% based on recovered starting material, which corresponds to 10% when accessed through the theoretical maximum yield achievable from the lignin content of beech sawdust. A full characterization of the molecular motor was performed (see ESI†). Notably, only the *E* (*R*,*R*) isomer (conglomerate) was formed, as confirmed by the crystal structure (Scheme 1).The molecular motor **7** was still pure and stable after 2.5 years of storage in darkness under air at room temperature, without effects on the reproducibility of its photoresponsive behaviour.

**Table 1** Justification of principles of green chemistry. Relevant principles of green chemistry and analysis for the synthesis of the first molecular motor from lignocellulose[45,46]

| Principles | Justification |
|---|---|
| Prevention of waste | As the synthesis of **7** from renewables was conducted predominantly using catalytic methods, stoichiometric amounts of waste could be minimized. Solvent intense column chromatography was omitted until the last step and replaced by precipitation and pH selective extraction (**3**). |
| Atom economy | Several important functional groups are inherently present in the lignin-derived platform molecule, leading to the synthesis of **7** in just six benign steps, increasing the overall atom-economy. In future optimizations the excess of isobutyraldehyde (2 eq.) could be decreased, but was out of the scope of the proof of concept paper. Dimethyl carbonate (DMC) is acting as a renewable, environmentally benign, low-toxicity methylating agent and solvent,[42] which could be recycled by evaporation. |
| Less hazardous chemical synthesis | The synthetic routes starting from the platform chemical 4-(3-hydroxypropyl)-2,6-dimethoxyphenol (dihydrosynapyl alcohol) **1** were designed to provide the compound in a straightforward fashion, preferably in catalytical reactions. In the oxidation step from **2** to **3** catalytic amounts of $Fe^{3+}$ are used instead of stoichiometric amounts of $Cr^{6+}$. Eaton's reagent utilizing the synergistic combination of $P_2O_5$ with Methanesulfonic acid in the Friedel–Crafts acylation step was chosen to decrease the use of polyphosphoric acid. |
| Benign solvents and auxiliaries | Environmentally benign and only non-halogenated solvents (water, methanol, ethyl acetate) were used throughout the synthesis and purification of motor precursor **6**.In the oxidation step, ethyl acetate (EtOAc) was used as an alternative benign solvent instead of 1,2-dichloroethane (DCE), which is commonly used in similar oxidation procedures.[43] |
| Use of renewable feedstocks | All atoms in the whole synthesis pathway can potentially be sourced from renewables and *via* their respective bio-derived platform chemicals. Specifically, the aromatic platform chemical 4-(3-hydroxypropyl)-2,6-dimethoxyphenol (dihydrosynapyl alcohol) **1** can be directly obtained from lignocellulose *via* a reductive catalytic fractionation strategy.[12] Dimethyl carbonate (DMC) as a potentially renewable, environmentally benign, low-toxicity methylating agent and solvent[42] provided the trimethoxy compound **2** (93% yield). The crucial stereogenic centre was introduced in an aldol condensation of **4** with isobutyraldehyde in water yielding the corresponding olefin 5,6,7-trimethoxy-2-(2-methylpropylidene)-2,3-dihydro-1H-inden-1-one **5**, followed by quantitative hydrogenation to afford **6**. |
| Reduce derivatives | Derivatization is avoided by direct oxidation of compound **2** to compound **3** with $O_2$. The whole synthesis towards the molecular motor **7** was conducted without the use of protecting groups. |
| Catalysis | Four out of six steps were run in a catalytic fashion, using $K_2CO_3$, $Fe(NO_3)_3$, TEMPO, KCl as benign catalysts. In the oxidation step from **2** to **3** catalytic amounts of $Fe^{3+}$ are used instead of stoichiometric amounts of $Cr^{6+}$. The methylation of **1** to **2** was conducted *via* a catalytic dimethyl carbonate route without the production of equimolar amounts of inorganic waste. |

 

The overall synthetic procedure assessment based on the criteria of the *12 Principles of Green Chemistry* is presented in Table 1.

### Photoisomerisation

UV/Vis and $^1$H-NMR spectroscopies and computational analysis were used to determine the rotation properties of the overcrowded alkene 7. Fig. 3A depicts the observed unidirectional rotation cycle for molecular motor 7.

As typical for the photochemical behaviour observed in first generation rotary motors,[17] upon light irradiation $E^s$-7 forms the corresponding $Z^u$ isomer (for the complete cycle, see Fig. 3A). This unstable state could either be switched back upon irradiation with longer wavelengths or perform a THI to reach the stable $Z$ state ($Z^s$-7). This step is predicted to be thermodynamically feasible at the ωB97X-D3BJ/def2-TZVP//r$^2$SCAN-3c level,[47–49] with a $\Delta G$ of −11.5 kcal mol$^{-1}$ and a $\Delta G^{\ddagger}$ of 19.2 kcal mol$^{-1}$. The $Z^u \rightarrow Z^s$ kinetic barrier is predicted to be lower relatively to other first-generation motors.[20] These values are associated with a process that can happen instantaneously at room temperature. Irradiation of the so-formed $Z^s$-7 leads to the unstable $E$ isomer ($E^u$-7), which repopulates the initial $E^s$-7 with a second THI. The predicted $\Delta G$ for this step (−6.9 kcal mol$^{-1}$) supports the motor function, while the

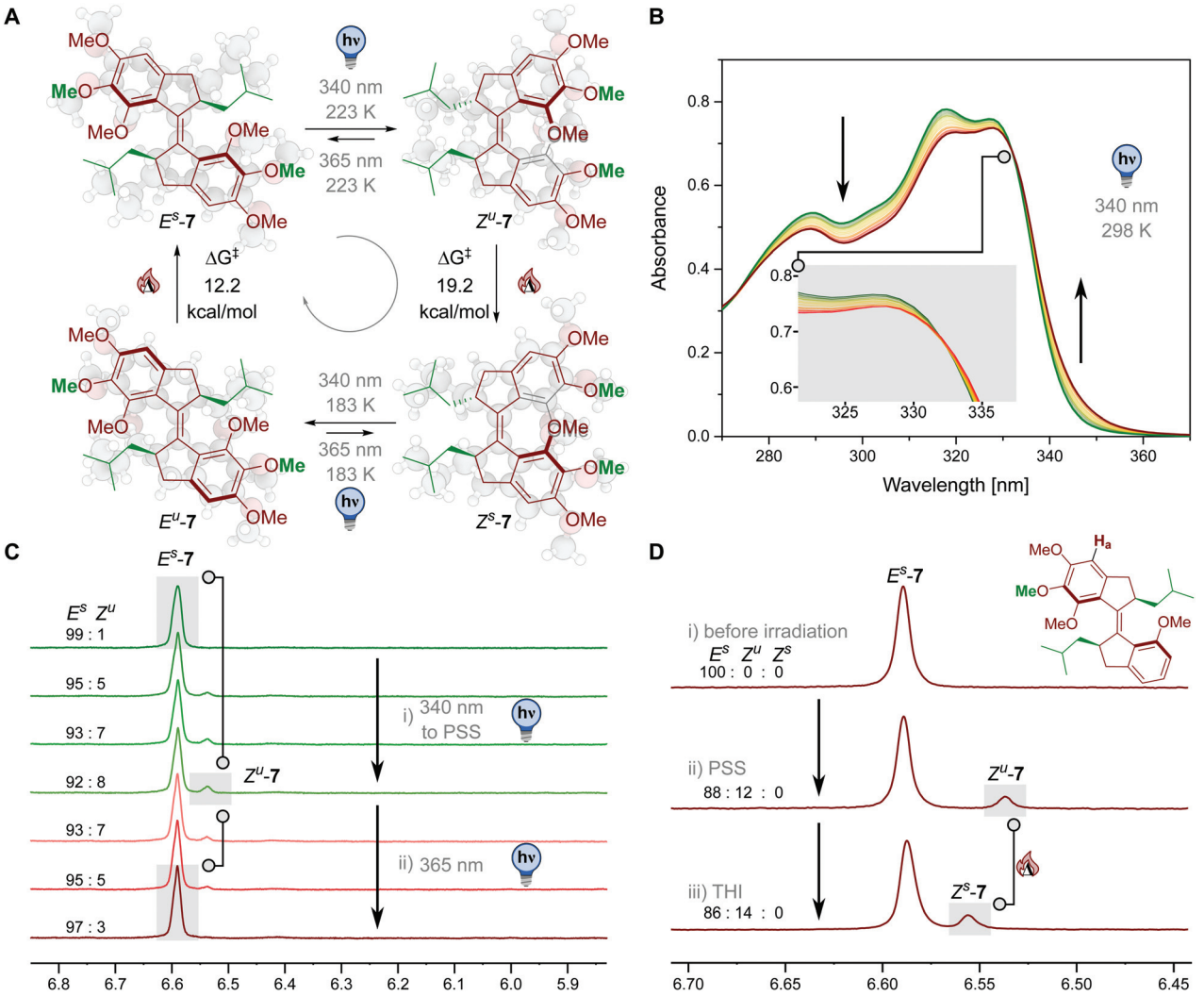


**Fig. 3** (A) Four state rotary cycle of compound 7. The molecular geometries and Gibbs Free Energies of activations are computed at the ωB97X-D3BJ/def2-TZVP//r$^2$SCAN-3c level. (B) UV/Vis absorption spectrum of $E^s$-7 recorded at 298 K in degassed $CH_2Cl_2$ (DCM, 2 × 10$^{-3}$ M, $N_2$) upon irradiation with a $\lambda_{irr}$ = 340 nm LED. The inset shows a close-up of the isosbestic point. (C) $^1$H-NMR spectrum (500 MHz, 223 K) of the aromatic region, showcasing proton $H_a$ of 7 measured in degassed DCM-$d_2$ (3.9 × 10$^{-3}$ M). (i) First irradiation to its PSS with a Thorlabs $\lambda_{irr}$ = 340 nm LED coupled to a 600 μm optical fibre, which led the light into the NMR tube inside the spectrometer, was carried out, PSS: 120 min, $PSS_{340}$ ratio: 92 : 8 ($E^s$ : $Z^u$). (ii) Spectral changes upon irradiation with a Thorlabs $\lambda_{irr}$ = 365 nm LED coupled to a 600 μm optical fibre are displayed. (D) $^1$H-NMR spectrum (500 MHz, 223 K) of the aromatic region, showcasing proton $H_a$ of 7 recorded in degassed DCM-$d_2$ (4.2 × 10$^{-3}$ M). First irradiation to its PSS with a Thorlabs $\lambda_{irr}$ = 340 nm LED coupled to a 600 μm optical fibre, which led the light into the NMR tube inside the spectrometer, $PSS_{340}$ ratio: 88 : 12 ($E^s$ : $Z^u$). The NMR tube was allowed to heat up to 298 K for 30 min to induce thermal helix inversion and measured again. (i) Initial state ($E^s$), (ii) Photoisomerization to unstable state (PSS $ratio_{340}$: 88 : 12 ($E^s$ : $Z^u$)) and (iii) thermal helix inversion ($ratio_{THI}$: 88 : 12 ($E^s$ : $Z^s$)).

predicted activation barrier ($\Delta G^{\ddagger}$ = 12.2 kcal mol$^{-1}$) suggests also in this case a fast step, in which the THI barrier prevents direct observation of the unstable $E^u$-7 state at room temperature. The predicted cycle of the motor suggests a continuous rotation upon light irradiation at room temperature, when photostationary state between $E^s$- and $Z^s$-7 is reached. The lowered thermal barriers are a possible consequence of the limited steric hindrance offered by the methoxy groups in the *fjord* region, a less bulky alternative to the methyl groups of the more classic design (Fig. 2). The unidirectional, continuous motion at room temperature of a molecular photoactuator is a key property for potential applications of these structures in more complex molecular machineries.

We confirmed our predictions following the irradiation of motor $E^s$-7 *via* UV/Vis spectroscopy (see Fig. 3B and a more detailed discussion in the ESI†). Irradiating a solution of motor $E^s$-7 in DCM we could observe the decrease of the main ππ* band and the rise of a tail shifted bathochromically. After reaching the PSS population, when no more changes in the spectra could be observed, we noted that no more changes in the spectrum could be induced by thermal or photochemical means (see ESI†). We consequently assigned the signal of the new species appearing in the UV/Vis spectrum to the stable $Z^s$ state, since the unstable states are thermally too unstable to be observed at room temperature or at −5 °C.[50] These findings are consistent with the observed isosbestic point, which are indicative of an apparent direct monomolecular interconversion between $E^s$-7 and $Z^s$-7, a feature already observed in four-state unidirectional motors with low THI barriers at ambient temperature.

We also carried out the photoisomerization studies of 7 at room temperature in $^1$H-NMR in DMSO-$d_6$ and DCM-$d_2$ ($\lambda_{irr}$ = 340 nm, Fig. S7–S12†). Isomerization from $E^s$ to $Z^s$ took place, but as expected neither unstable $Z^u$ nor $E^u$ could be obtained (upon irradiation with $\lambda_{irr}$ = 340 nm/365 nm or thermally), supporting our hypothesis. The PSS ratios of the different isomers of 7 were determined by averaging the integrals of the aromatic proton $H_a$ (see Fig. 3D). These observations are consistent with the results from the UV/Vis experiments. Subsequently, we studied the photoisomerization behaviour of 7 at low temperature. Upon irradiation of stable *E*-7 in DCM-$d_2$ with $\lambda_{irr}$ = 340 nm UV light at 223 K, formation of a new isomer could be observed (Fig. S13–S15†). Comparison with similar first generation motors suggested that this isomer could be $Z^u$,[38] which was confirmed by irradiation of the sample with $\lambda_{irr}$ = 365 nm UV light, leading to back isomerisation at low temperature (223 K) to the stable $E^s$ isomer (Fig. 3C, S14 and S15†). In a follow-up experiment, $Z^u$ was populated at low temperature in identical fashion (223 K, 340 nm) and the solution allowed to heat up to 298 K for 30 min, showing THI from $Z^u$ to $Z^s$ quantitatively, proving the consistency of the isomerization mechanism with first generation motors. (Fig. 3D and S16–S18†). Photoisomerization studies of stable $Z^s$ at low temperature (223 K, $\lambda_{irr}$ = 340 nm, S19–S21†) resulted in a spectrum showing a mixture of $E^s : Z^u : Z^s$ (83 : 9 : 8). Hence the photoisomerization of stable $Z^s$ at 183 K ($\lambda_{irr}$ = 340 nm and Fig. S22†) was performed to detect unstable $E^u$-7. At this temperature we could observe the formation of a shoulder in the signal attributed to $E^s$-7 in the $H_a$ region. Applying peak deconvolution analysis we could qualitatively assign the shoulder to $E^u$-7, as the relative position of the signal is consistent with previously reported first generation molecular motors (see ESI†).[36,50,51]

The data we obtained on photoisomerization and fast thermal helix inversion of 7 are consistent with a first-generation molecular motor capable of performing continuous unidirectional rotation at room temperature. This example shows that by utilizing a green methodology, the late-stage alkylation of the alpha carbon offers a lot of potential for synthesizing libraries of molecular motors obtained from renewable feedstock.

## Conclusions

This article describes the modular synthesis of a molecular motor 7, synthetized for the first time exclusively from renewable building blocks: lignin derived **1** (dihydrosinapyl alcohol/4-(3-hydroxypropyl)-2,6-dimethoxyphenol), dimethyl carbonate and isobutyraldehyde with an overall yield of 15% based on recovered starting material. Since dimethyl carbonate and isobutyraldehyde can be obtained from $CO_2$ *via* chemical and biochemical catalytic procedures respectively, our molecular motor can be sourced entirely from renewable feedstock.[39,40,52] By utilizing the inherently present functional groups, the synthesis of 7 was realized in just six environmentally benign steps, such as methylation with dimethyl carbonate, catalytic oxidation with molecular oxygen, metal-free Friedel–Crafts acylation, aldol condensation and hydrogenation sequence. Furthermore, environmentally benign and only non-halogenated solvents were used throughout the synthesis and purification. Solvent intense column chromatography was omitted until the last step and replaced by precipitation and pH selective extraction. The absolute configuration of **5** and 7 was determined from crystal structure *via* XRD. This investigation demonstrates that highly complex, high-value target molecules such as rotary molecular motors can be synthesized from renewable resources. In addition, motor 7 can undergo a full 360° rotation at room temperature following a single light stimulus, thanks to the low thermal helix inversion barriers. This property is particularly sought after in molecular motors, envisaging their application in a system that requires continuous motion such as the already mentioned targeted drug delivery systems, responsive coatings for self-healing surfaces, paints and resins or muscles for soft robotics.

The modular synthesis we employed enables the functionalization of the phenol moiety, which is in the same position where previous switchable catalysts were functionalized, enabling the creation of photoresponsive molecular catalyst libraries.[53–55] As a general strategy it opens pathways for future machines, motors and nanoscience made from sustainable sources. Future molecular machines can take advantage from the application of the principles of Green Chemistry in

 

the synthesis and purification. Achieving such synthesis will benefit the environment and decrease expenses related to hazardous waste management.

## Author contributions

Thomas Freese: conceptualization, data curation, formal analysis, investigation, validation, visualization, writing – original draft, Bálint Fridrich: conceptualization, data curation, formal analysis, investigation, methodology, visualization, writing – original draft, Stefano Crespi: conceptualization, data curation, formal analysis, visualization, writing – review & editing, Anouk S. Lubbe: conceptualization, writing – review & editing, Katalin Barta: conceptualization, funding acquisition, supervision, writing – review & editing, Ben L. Feringa: conceptualization, funding acquisition, supervision, writing – review & editing

## Conflicts of interest

There are no conflicts to declare.

## Acknowledgements

This work was supported financially by the European Research Council (ERC, Starting Grant 2015 (CatASus) 638076 to K.B.) and the Ministry of Education, Culture and Science of the Netherlands (Gravitation Program no 024.001.035 to B.L.F.). The authors thank Anirban S. Mondal (University of Groningen) and Folkert de Vries (University of Groningen) for the measurement and refinement of the crystal structures. Hans van der Velde (University of Groningen) for performing Elemental Analysis and Renze Sneep (University of Groningen) for high resolution mass spectrometry measurements are gratefully acknowledged. The authors thank Xianyuan Wu (University of Groningen) for donation of the starting material 4-(3-hydroxypropyl)-2,6-dimethoxyphenol **1**.

## References

1 Z. Sun, B. Fridrich, A. De Santi, S. Elangovan and K. Barta, *Chem. Rev.*, 2018, **118**, 614.
2 W. Schutyser, T. Renders, S. Van Den Bosch, S. F. Koelewijn, G. T. Beckham and B. F. Sels, *Chem. Soc. Rev.*, 2018, **47**, 852.
3 Y. M. Questell-Santiago, M. V. Galkin, K. Barta and J. S. Luterbacher, *Nat. Rev. Chem.*, 2020, **4**, 311.
4 M. V. Galkin and J. S. M. Samec, *ChemSusChem*, 2016, **9**, 1544.
5 M. M. Abu-Omar, K. Barta, G. T. Beckham, J. S. Luterbacher, J. Ralph, R. Rinaldi, Y. Román-Leshkov, J. S. M. Samec, B. F. Sels and F. Wang, *Energy Environ. Sci.*, 2021, **14**, 262.
6 Q. Meng, J. Yan, R. Wu, H. Liu, Y. Sun, N. N. Wu, J. Xiang, L. Zheng, J. Zhang and B. Han, *Nat. Commun.*, 2021, **12**, 1.
7 Y. Liao, S. F. Koelewijn, G. van den Bossche, J. van Aelst, S. van den Bosch, T. Renders, K. Navare, T. Nicolaï, K. van Aelst, M. Maesen, H. Matsushima, J. M. Thevelein, K. van Acker, B. Lagrain, D. Verboekend and B. F. Sels, *Science*, 2020, **367**, 1385.
8 S. S. Wong, R. Shu, J. Zhang, H. Liu and N. Yan, *Chem. Soc. Rev.*, 2020, **49**, 5510.
9 S. Elangovan, A. Afanasenko, J. Haupenthal, Z. Sun, Y. Liu, A. K. H. Hirsch and K. Barta, *ACS Cent. Sci.*, 2019, **5**, 1707.
10 M. Pelckmans, T. Renders, S. Van De Vyver and B. F. Sels, *Green Chem.*, 2017, **19**, 5303.
11 A. Afanasenko and K. Barta, *iScience*, 2021, **24**, 102211.
12 Z. Sun, G. Bottari, A. Afanasenko, M. C. A. Stuart, P. J. Deuss, B. Fridrich and K. Barta, *Nat. Catal.*, 2018, **1**, 82.
13 N. Koumura, R. W. J. Zijistra, R. A. Van Delden, N. Harada and B. L. Feringa, *Nature*, 1999, **401**, 152.
14 B. L. Feringa, W. F. Jager, B. de Lange and E. W. Meijer, *J. Am. Chem. Soc.*, 1991, **113**, 5468.
15 B. L. Feringa, *Acc. Chem. Res.*, 2001, **34**, 504.
16 J. E. McMurry, M. G. Silvestri, M. P. Fleming, T. Hoz and M. W. Grayston, *J. Org. Chem.*, 1978, **43**, 3249.
17 S. Kassem, T. Van Leeuwen, A. S. Lubbe, M. R. Wilson, B. L. Feringa and D. A. Leigh, *Chem. Soc. Rev.*, 2017, **46**, 2592.
18 C. Pezzato, C. Cheng, J. F. Stoddart and R. D. Astumian, *Chem. Soc. Rev.*, 2017, **46**, 5491–5507.
19 J. C. M. Kistemaker, A. S. Lubbe and B. L. Feringa, *Mater. Chem. Front.*, 2021, **5**, 2900.
20 D. R. S. Pooler, A. S. Lubbe, S. Crespi and B. L. Feringa, *Chem. Sci.*, 2021, 14964.
21 K. Y. Chen, O. Ivashenko, G. T. Carroll, J. Robertus, J. C. M. Kistemaker, G. London, W. R. Browne, P. Rudolf and B. L. Feringa, *J. Am. Chem. Soc.*, 2014, **136**, 3219.
22 R. Eelkema, M. M. Pollard, N. Katsonis, J. Vicario, D. J. Broer and B. L. Feringa, *J. Am. Chem. Soc.*, 2006, **128**, 14397.
23 J. Hou, A. Mondal, G. Long, L. de Haan, W. Zhao, G. Zhou, D. Liu, D. J. Broer, J. Chen and B. L. Feringa, *Angew. Chem., Int. Ed.*, 2021, **60**, 8251.
24 I. Aprahamian, *ACS Cent. Sci.*, 2020, **6**, 347.
25 Y. Shirai, K. Minami, W. Nakanishi, Y. Yonamine, C. Joachim and K. Ariga, *Jpn. J. Appl. Phys.*, 2016, **55**, 1102A2.
26 F. Lancia, A. Ryabchun and N. Katsonis, *Nat. Rev. Chem.*, 2019, **3**, 536.
27 A. Ryabchun, F. Lancia, J. Chen, D. Morozov, B. L. Feringa and N. Katsonis, *Adv. Mater.*, 2020, **32**, 1.
28 J. Chen, F. K. C. Leung, M. C. A. Stuart, T. Kajitani, T. Fukushima, E. Van Der Giessen and B. L. Feringa, *Nat. Chem.*, 2018, **10**, 132.
29 M. Kathan, S. Crespi, N. O. Thiel, D. L. Stares, D. Morsa, J. de Boer, G. Pacella, T. van den Enk, P. Kobauri,

G. Portale, C. A. Schalley and B. L. Feringa, *Nat. Nanotechnol.*, 2022, **17**, 159.
30 R. F. Ludlow and S. Otto, *Chem. Soc. Rev.*, 2008, **37**, 101.
31 A. C. Coleman, J. M. Beierle, M. C. A. Stuart, B. Maciá, G. Caroli, J. T. Mika, D. J. Van Dijken, J. Chen, W. R. Browne and B. L. Feringa, *Nat. Nanotechnol.*, 2011, **6**, 547.
32 D. J. Van Dijken, J. Chen, M. C. A. Stuart, L. Hou and B. L. Feringa, *J. Am. Chem. Soc.*, 2016, **138**, 660.
33 J. J. D. De Jong, L. N. Lucas and R. M. Kellogg, *Science*, 2004, **304**, 278.
34 B. L. Feringa, *Angew. Chem., Int. Ed.*, 2017, **56**, 11060.
35 R. A. Sheldon, *Chem. Soc. Rev.*, 2012, **41**, 1437.
36 M. M. Pollard, A. Meetsma and B. L. Feringa, *Org. Biomol. Chem.*, 2008, **6**, 507.
37 D. Roke, S. J. Wezenberg and B. L. Feringa, *Proc. Natl. Acad. Sci. U. S. A.*, 2018, **115**, 9423.
38 M. M. Pollard, P. V. Wesenhagen, D. Pijper and B. L. Feringa, *Org. Biomol. Chem.*, 2008, **6**, 1605.
39 S. Atsumi, W. Higashide and J. C. Liao, *Nat. Biotechnol.*, 2009, **27**, 1177.
40 S. Fang and K. Fujimoto, *Appl. Catal., A*, 1996, **142**, 8.
41 W. Lan, M. T. Amiri, C. M. Hunston and J. S. Luterbacher, *Angew. Chem., Int. Ed.*, 2018, **57**, 1356.
42 G. Fiorani, A. Perosa and M. Selva, *Green Chem.*, 2018, **20**, 288.
43 X. Jiang, J. Zhang and S. Ma, *J. Am. Chem. Soc.*, 2016, **138**, 8344.
44 H. Cho and S. Matsuki, *Heterocycles*, 1996, **43**, 127.
45 P. T. Anastas and J. C. Warner, *Green Chemistry: Theory and Practice*, Oxford University Press, New York, 1998.
46 J. B. Zimmerman, P. T. Anastas, H. C. Erythropel and W. Leitner, *Science*, 2020, **367**, 397.
47 S. Grimme, A. Hansen, S. Ehlert and J. M. Mewes, *J. Chem. Phys.*, 2021, **154**, 064103.
48 J. Da Chai and M. Head-Gordon, *Phys. Chem. Chem. Phys.*, 2008, **10**, 6615.
49 F. Weigend and R. Ahlrichs, *Phys. Chem. Chem. Phys.*, 2005, **7**, 3297.
50 D. R. S. Pooler, R. Pierron, S. Crespi, R. Costil, L. Pfeifer, J. Léonard, M. Olivucci and B. L. Feringa, *Chem. Sci.*, 2021, **12**, 7486.
51 D. Roke, M. Sen, W. Danowski, S. J. Wezenberg and B. L. Feringa, *J. Am. Chem. Soc.*, 2019, **141**, 7622.
52 G. A. Olah, *Angew. Chem., Int. Ed.*, 2005, **44**, 2636.
53 M. Vlatkovic, L. Bernardi, E. Otten and B. L. Feringa, *Chem. Commun.*, 2014, **50**, 7773.
54 D. Zhao, T. M. Neubauer and B. L. Feringa, *Nat. Commun.*, 2015, **6**, 6652.
55 E. Moulin, L. Faour, C. C. Carmona-Vargas and N. Giuseppone, *Adv. Mater.*, 2020, **32**, 1.

 